

Monte Carlo particle simulation of a quantum well heterojunction field-effect transistor: Comparison with experimental data

C. Moglestue

Citation: [Journal of Applied Physics](#) **80**, 1499 (1996); doi: 10.1063/1.363020

View online: <http://dx.doi.org/10.1063/1.363020>

View Table of Contents: <http://scitation.aip.org/content/aip/journal/jap/80/3?ver=pdfcov>

Published by the [AIP Publishing](#)

Articles you may be interested in

[Fabrication and characterization of modulation-doped-field-effect-transistors with antidot-patterned passivation layers](#)

Appl. Phys. Lett. **69**, 1924 (1996); 10.1063/1.117623

[Photo-Hall studies of modulation-doped field-effect transistors with short-period superlattice channels rather than alloy channels](#)

J. Vac. Sci. Technol. B **14**, 3350 (1996); 10.1116/1.588534

[Simulation of the capacitance–voltage characteristics of a single-quantum-well structure based on the self-consistent solution of the Schrödinger and Poisson equations](#)

J. Appl. Phys. **80**, 864 (1996); 10.1063/1.362895

[A composite quantum well field-effect transistor](#)

Appl. Phys. Lett. **69**, 85 (1996); 10.1063/1.118128

[Theoretical study of tunneling current in the access region of various heterojunction field-effect transistor structures](#)

J. Appl. Phys. **79**, 3603 (1996); 10.1063/1.361414

**SHIMADZU**
Excellence in Science

Powerful, Multi-functional UV-Vis-NIR and FTIR Spectrophotometers

Providing the utmost in sensitivity, accuracy and resolution for applications in materials characterization and nano research

- Photovoltaics
- Polymers
- Thin films
- Paints
- Ceramics
- DNA film structures
- Coatings
- Packaging materials

[Click here to learn more](#)

Four Shimadzu spectrophotometers are shown. From left to right: a small benchtop model, a larger benchtop model with a sample holder, a large floor-standing model with a large sample compartment, and a large floor-standing model with a large sample compartment and a control panel.

Monte Carlo particle simulation of a quantum well heterojunction field-effect transistor: Comparison with experimental data

C. Moglestue

Fraunhofer Institute of Applied Solid State Physics, Tullastrasse 72, D-79108 Freiburg, Germany

(Received 6 February 1996; accepted for publication 23 April 1996)

A heterojunction field-effect transistor with a quantum well channel has been studied using the Monte Carlo particle model. The transport in the channel has been calculated both considering and neglecting the effect of energy quantization of the conduction band. The results of the two approaches were found to agree well with each other and with experimental data. The significant differences between classical and quantum mechanical calculations are the better confinement of the carrier in the channel and the better agreement of the transfer characteristics with experiment for the latter. © 1996 American Institute of Physics. [S0021-8979(96)02115-9]

I. INTRODUCTION

The popular drift-diffusion, hydrodynamic, and parameter fitting modelling of heterojunction field-effect transistors do not shed sufficient light into the details of transport of electrons in heterojunction transistors because the heterojunctions cannot be treated in a physically transparent manner. The former two types of models only make use of average drift velocities without considering any deviation from them. As only the carriers in the tail of the distribution can overcome the potential steps at the heterojunctions these models have to make use of tricks. The correct way of describing a transistor with heterojunction interfaces would be to solve Boltzmann's transport and Poisson's field equations simultaneously in time and space—when a narrow channel is present this set of equations should be augmented with Schrödinger's wave equation. This poses a formidable mathematical problem which cannot be solved analytically except in trivial cases. Fortunately, the Monte Carlo particle model represents an indirect way of finding the solution of these equations by considering the transport stochastically.¹ As this method consists of following the transport histories of individual particles in detail, it also yields a profound transport theoretical insight into the physics of the transistor we are studying.

The purpose of this article is to study a heterojunction field-effect transistor by means of the Monte Carlo particle model. The transistor has a 120 Å wide channel, where we expect the conduction band to split into subbands, this would necessitate a quantum mechanical treatment. We shall calculate the transfer characteristics and equivalent circuit of this transistor using a classical transport model—neglecting the splitting of the conduction band into subbands in the channel—and a quantum mechanical treatment considering this conduction band splitting. The transistor will be described in Sec. II, where we shall also outline the salient points of the simulation model very briefly. The results of our calculations will then be presented and compared with each other for the two models and with experimental data from our own laboratory in the proceeding section before a conclusion will be reached.

II. TRANSISTOR GEOMETRY AND MODEL

The geometry of the heterojunction field-effect transistor we are simulating is shown in Fig. 1. The cap layer is uniformly doped *n*-type at $2 \times 10^{24} \text{ m}^{-3}$; underneath the source and drain contact metallization this layer is assumed to extend through the undoped $\text{In}_{0.25}\text{Ga}_{0.75}\text{As}$ layer into the semi-insulating $\text{Al}_{0.2}\text{Ga}_{0.8}\text{As}$ layer in order to make contact with the channel. No barriers have been considered existing between the Ohmic contact regions and the rest of the transistor. This means that the particles can pass in and out of the Ohmic contact regions into any material without encountering barriers. The Ohmic contacts are manufactured by diffusing metal into the semiconductor making the transition from alloy to semiconductor diffuse, we therefore treat the contact semiconductor transition as described because any details of the diffusion profile are not well known. The conduction band discontinuities at the heterojunctions elsewhere have been calculated from Krijn-van der Walle theory.^{2,3}

Transistors of near enough the same geometry have been manufactured in our laboratory.⁴ The GaAs layer above the $\text{In}_{0.25}\text{Ga}_{0.75}\text{As}$ channel contains an atomic silicon supply layer. On top of it, there are a 30 Å GaAs layer and a 30 Å $\text{Al}_{0.2}\text{Ga}_{0.8}\text{As}$ serving as etch stop layer ensuring uniform gate recess depth over the entire wafer. The gate recess is excavated by a dry etch down to the etch stop followed by a wet etch through it.⁴

The Monte Carlo particle modeling consists of following individual particles in detail. The transport of electrons consists of free flights terminated by scattering. The duration of these flights and the type of scattering ending them are distributed stochastically, the transport histories are calculated by selecting random numbers of the same respective distribution. When a particle wishes to cross a heterojunction interface, it is vetted whether it has sufficient kinetic energy associated with the motion perpendicular to it to overcome the potential step generated by the discontinuity in the conduction band; this discontinuity, however, is different whether the particle resides in a Γ , an *X*, or an *L* minimum. If this energy is sufficient, or there is a potential step down, this kinetic energy component is adjusted according to the step conserving the total energy, otherwise the particle experiences a specular reflection. An electron cannot shift from one

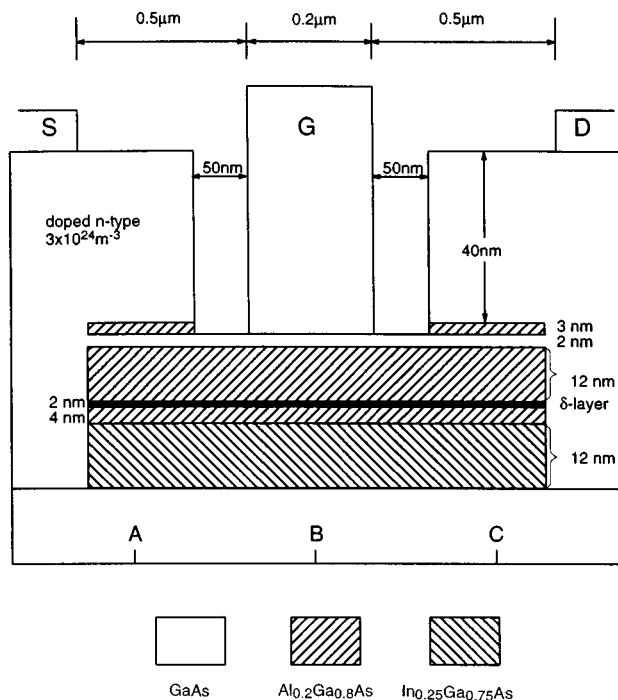


FIG. 1. Geometry of simulated heterojunction field-effect transistor. The Ohmic contact areas are considered as being GaAs n -type doped areas with a doping density equal to that of the cap layer and there are no barriers at their boundaries. A, B, and C indicate the positions where the band structure profiles in Fig. 2 have been shown. The δ -doping sheet density is $3.6 \times 10^{-16} \text{ m}^{-2}$.

energy minimum to another, this is only considered possible by mediation of a phonon.

In the quantum well, the energy associated with the momentum perpendicular to it and the corresponding energy are only allowed a set of discrete values. A particle is caught in the well by a scattering event rendering its momentum perpendicular to the well one of these allowed values. Although the energy levels are sharp, the scattering rates into the wells between the different energy levels and out of the wells are comparable to the corresponding bulk rates. The energy levels will vary with the width of the well, however, we consider the well being uniformly thick. The perpendicular electric field along the channel, Fig. 2, also causes the energy levels to vary about 10 meV along the channel, we consider this variation sufficiently small compared to the level separation to justify using average levels for each of them. All energy levels are included in our model. On capture, the total kinetic energy of the captured particle may still be greater than the energy representing the depth of the well, in this case there is a great chance that the next scattering event will liberate the particle from the well. Above the well the energy levels are quasicontinuous and the scattering is bulk like.

In our simulation, the field equation is solved every 2 ps over a rectangular regular grid of 1 by 7 nm², with the latter dimension along the length of the channel. This choice is fine enough to consider our solution of Poisson's equation quasicontinuous in space and time. In the classical model, quantization of the energy in the channel is not considered, in the quantum mechanical case the wave equation is solved only

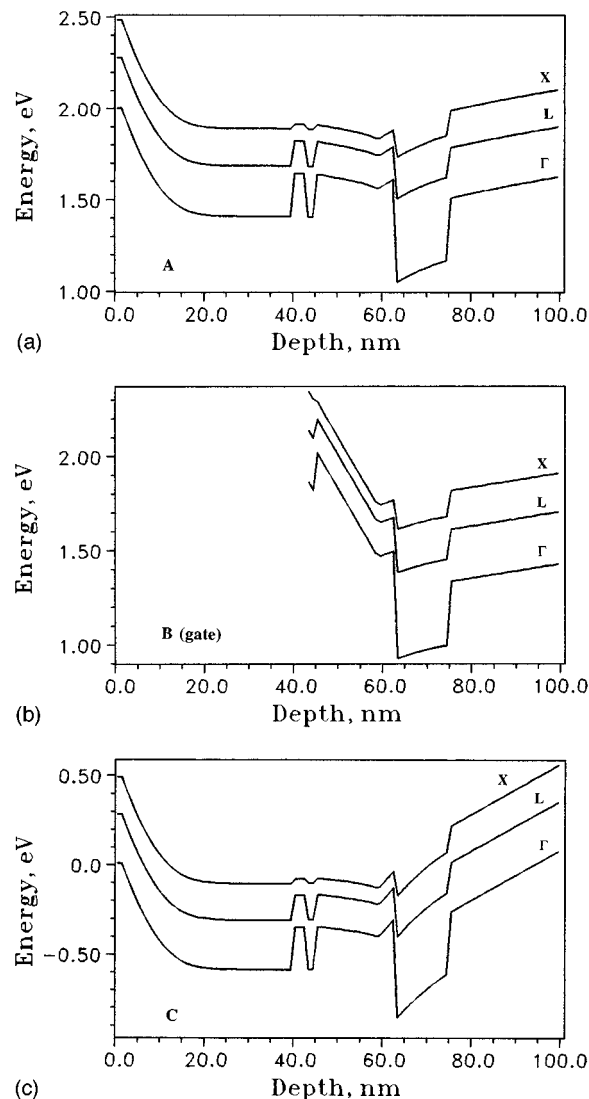


FIG. 2. Calculated band structures during steady state at vertical sections through the transistor at positions A, B, and C in Fig. 1. The curves represent the band structure at the band minima at the Γ , X, and L points of the Brillouin zone. Drain voltage: 2 V; gate potential -0.4375 V .

once during steady state for the average electric field. The solution is repeated for each set of chosen gate and drain potentials. Between the $\text{Al}_{0.2}\text{Ga}_{0.8}\text{As}$ etch stop and the $\text{Al}_{0.2}\text{Ga}_{0.8}\text{As}$ layer containing the δ -doped supply layer there is another GaAs 30 Å quantum well. This is so narrow that the first level lies near the top of the well so that quantum transport needs not be considered. The atomic width δ -layer also forms a well with only one level on top of it so that the layer in which it is embedded behaves like bulk.

Poisson's field equation is solved with fixed potentials at the contacts and zero field gradient at the boundaries of the simulation area. The substrate is semi-insulating, where we consider the Fermi level being pinned at the center of the band gap, this means that the potential there will be about -0.75 V . In our calculations, the potential at the bottom of the simulation area has been set to the Schottky contact potential.

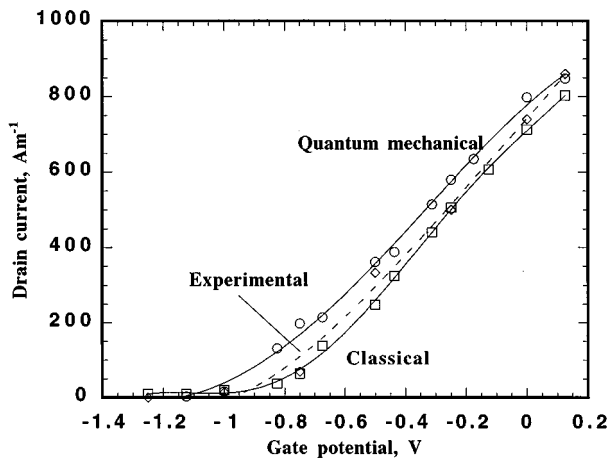


FIG. 3. Transfer characteristics of the heterojunction field-effect transistor at 2 V drain bias for classical (lower curve) and the quantum mechanical transport model (upper curve) compared with the measured intrinsic characteristic at a drain bias of 1.5 V (dashed). The gate potential includes the Schottky contact potential of -0.75 V; the corresponding laboratory voltage can be obtained by subtracting (algebraically) the Schottky potential, i.e., -0.75 V corresponds to 0 V in the laboratory.

III. THE TRANSFER CHARACTERISTICS

For each choice of drain and gate bias, the drain current is obtained by counting the net flow of particles through the drain during steady state. Apart from noisy fluctuations, the net injection of particles at the source balances the current at the drain, no gate current flows except at the most positive forward bias of the gate. The gate potential includes the Schottky contact potential which is taken to be -0.75 V. Figure 3 shows the drain current versus gate potential for 2 V drain bias. The corresponding gate bias is obtained by subtracting the Schottky contact potential, e.g., -0.75 V gate potential in the figure corresponds to a laboratory bias of zero. The currents are sampled during steady state over an interval of 8 ps. We have calculated transfer characteristics for both the classical and the quantum mechanical transport model and compared with measured results. The classical curve displays a softer gate threshold than the measured and quantum mechanical result.

Figure 4 shows that the quantum mechanical approach to the transport in the channel confines the electrons better to the channel than the classical approach. The explanation lies entirely in the scattering rates—the orthogonality of the wave functions for each energy level disfavors jumping between the levels so the electrons tend to be better confined. There is no significant difference in the distribution of the electric potential between the two descriptions, therefore only that of the quantum mechanical calculation is shown in Fig. 5. The results in these two figures have been obtained for a gate potential of -0.4375 V and drain bias of 2 V, which is a point near the maximum in the transconductance.

IV. MICROWAVE CHARACTERISTICS

The microwave characteristics have been calculated around a working point of -0.4375 V gate bias (inclusive of

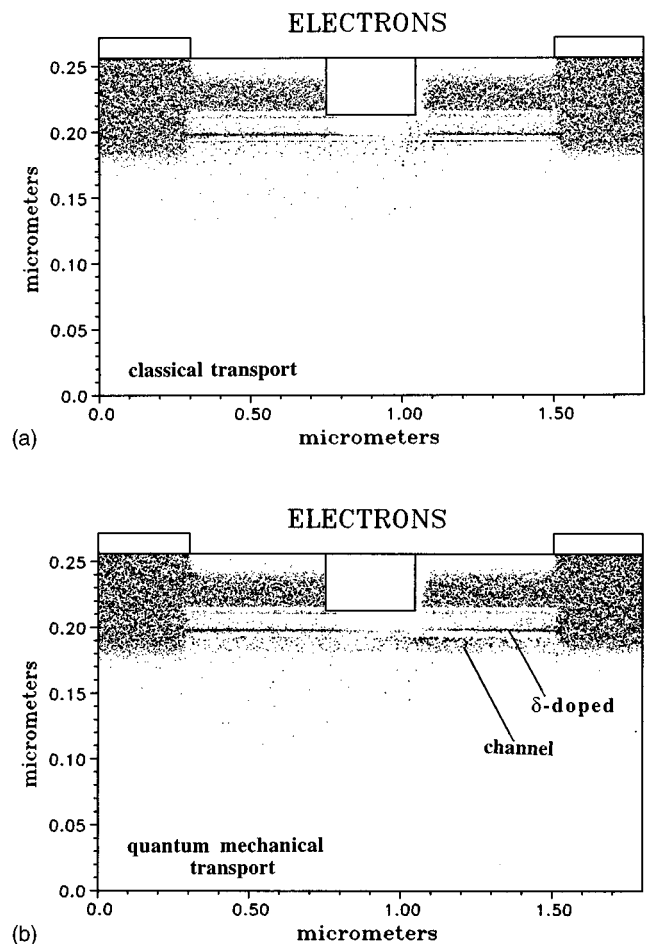


FIG. 4. Instantaneous distribution of electrons calculated using the (a) classical and the (b) quantum mechanical transport model. Gate potential: -0.4375 V (including the Schottky contact potential of -0.75 V), drain bias: 2 V.

the Schottky contact potential) or $+0.3125$ V laboratory bias and 2 V drain bias. The gate and drain bias have been incremented in turn by 0.125 and 1.0 V, respectively, from the working point and the current response of both the gate and

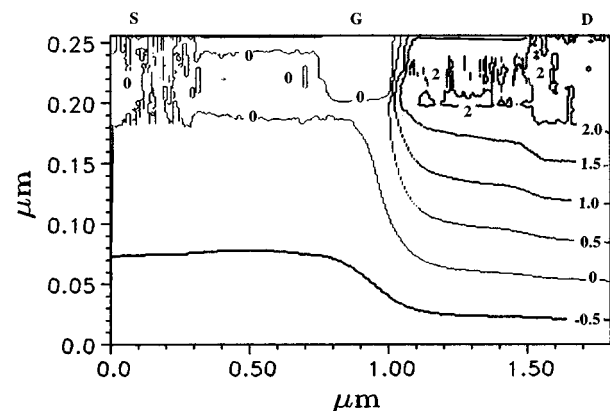


FIG. 5. Instantaneous distribution of the electric potential calculated from the quantum mechanical transport model. Gate potential: -0.4375 V (including the Schottky contact potential of -0.75 V), drain bias: 2 V. The irregularities in the equipotential lines are due to noise. The parameter represents the potential in volts.

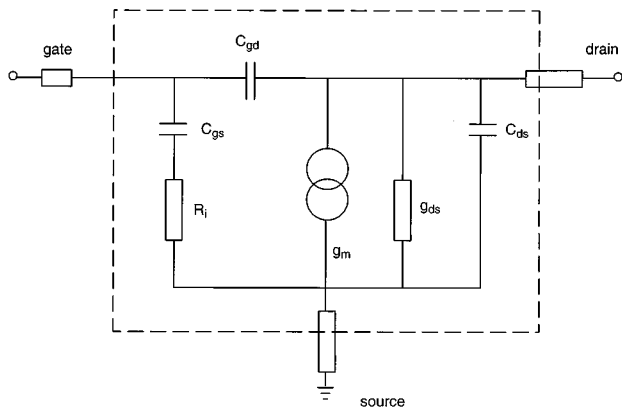


FIG. 6. Equivalent circuit of the transistor. The intrinsic part is inside the dashed rectangle; the output resistances at the source and drain have been drawn partly inside the intrinsic frame to symbolize that some of these resistances originate from bulk transport within the simulated part of the transistor.

the drain Fourier analyzed. The chosen increments are sufficiently small to be considered within a linear range of the steady state characteristics of the transistor yet large enough to minimize the error due to noise from the analysis. The currents consist of a particle and a displacement component which are recorded for each solution of the field equation. The Fourier analyzed signals yield the four y parameters $y_{ij} = \partial I_i / \partial V_j$ where $i, j = 1$ stands for gate and 2 for drain.^{1,5} The y parameters give the relation between the gate and drain currents and the gate and drain voltages as function of frequency, and from the equivalent circuit of Bosch and Berroth.⁶ In Fig. 6, we get the six equivalent circuit parameter and the transit time (see Table I).

V. COMPARISON WITH EXPERIMENTAL DATA

The forward and transfer characteristics have been measured in house on transistors of near enough the same geometry as we have calculated. The dc characteristics have been obtained using a Hewlett Packard (HP) 4145 semiconductor parameter analyzer. Our calculated results have been obtained neglecting any effect of trapping, the comparison is meaningful because the aluminum contents is so low that the EL2 centers will not be active. The s parameters, from which the equivalent circuit has been extracted, have been measured at an HP 8510 C based network analyzer for frequencies up to 120 GHz.⁷

The Monte Carlo particle model yields the intrinsic properties of the transistor, this means that the transport in the resistive metallization of the contacts, contact pads, and the leads have not been considered. Measuring the transistors, these resistances are included, in other words we measure the extrinsic characteristics. To compare, it is therefore necessary to correct for the external resistances. The external resistances in metallization, bond pads, and leads are represented by the resistance at source, gate and drain in Fig. 6. The linear part of the forward characteristics of the transistor below the knee represents the sum of the internal and external resistances. In addition to the internal resistance R_i , we also have resistances in the source and drain regions due to

TABLE I. Calculated and experimental equivalent circuit parameters.

Parameter	Classical transport	Quantum mechanical	Experimental
C_{gd} (pF m ⁻¹)	35	42	90
C_{gs} (pF m ⁻¹)	640	590	1000
C_{ds} (pF m ⁻¹)	310	324	300
R_i (10 ⁻⁴ Ω m)	3.2	4.7	4
g_m (S m ⁻¹)	920	1010	1050
g_{ds} (S m ⁻¹)	9	17	45
τ (ps)	0.75	0.38	0.33

bulk scattering there. These resistances are in series with the external ones. This has been symbolized in Fig. 6 by letting the boundary of the intrinsic transistor cross the symbols for them. From the calculated forward characteristics, shown in Fig. 7, we get a resistance of 5.3×10^{-4} Ω m below the knee and the corresponding measured resistance from Fig. 8 of 12.5×10^{-4} Ω m. The difference, $R_{ext} = 7.2 \times 10^{-4}$ Ω m, represents the external resistances, the part of the resistances outside the dashed rectangle in Fig. 6.

The correction in the transconductance is

$$g_{m,int} = g_{m,ext} / (1 - g_{m,ext} R_{ext}),$$

which applied to the observed transconductance shown in Fig. 9 yields the value quoted in Table I. The intrinsic experimental transfer characteristic drawn in Fig. 3 has been obtained from the measured one shown in Fig. 9 by applying the above formula with $g_{m,ext}$ replaced by the extrinsic current values.

There is no significant difference between the equivalent circuit parameters calculated from a classical and a quantum mechanical transport model. In comparison with experimental data, we notice that our calculated values for C_{gd} are about half of the measured one. The reason for that is that we have only simulated that part of the transistor which is nearest to the gate; the source and drain metallization extends micrometers in both directions away from the gate, this also

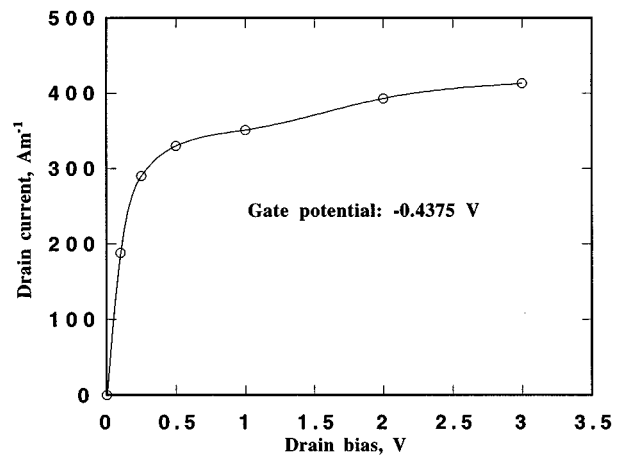


FIG. 7. Calculated forward characteristics for a gate potential of -0.4375 V (gate bias: $+0.3125$ V).

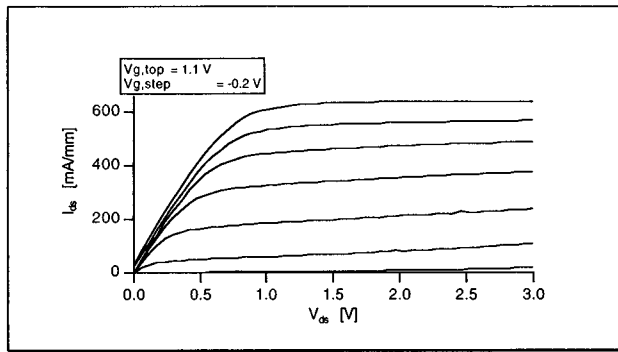


FIG. 8. Measured forward characteristics for gate biases from +1.1 to -0.1 V in steps of -0.2 V. Drain bias: 1.1 V.

contributes to C_{gd} . Our values for C_{gs} are also about half the experimental ones, probably for the same reason, but our C_{sd} are accurate.

The internal resistance, R_i , agrees well. The quantum mechanical value of the transconductance, g_m , is better than the one from classical theory; the transadmittance, g_{ds} however, is below in both models. Also the transit time, τ , are above the measured one although the quantum theoretical one falls nearest.

VI. CONCLUSION

Steady state and microwave characteristics of a heterojunction field-effect transistor have been calculated both considering and neglecting the division of the conduction band in the channel into subbands due to energy quantization. We have used the Monte Carlo particle model because it yields a self consistent solution in space and time of Boltzmann's transport, Poisson's field, and Schrödinger's wave equation. The results of our calculations have been compared with experimental data. Both the quantum mechanical and the classical transport results compare well with measured results and the only significant indication as to which model is most accurate lies in the steady state transfer characteristics, which

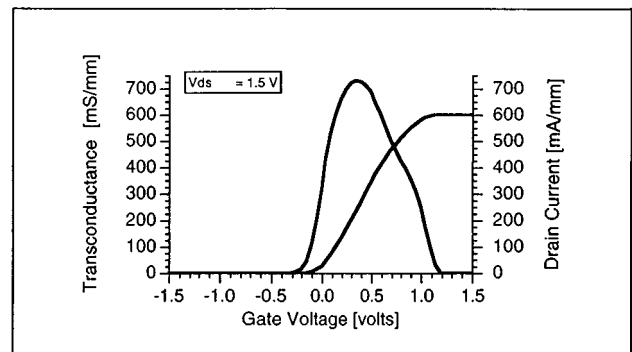


FIG. 9. Measured transfer characteristics and transconductance for 1.5 V drain bias.

like the laboratory data, show a better defined threshold gate voltage than that obtained from the classical approach. Also, from physical completeness, we consider a quantum mechanical approach to be better justified because of the quantization of the energy levels in the channel.

ACKNOWLEDGMENT

The author is indebted to the German Federal Ministry of Education and Research (BMBF) and of Defence (BMvG) for financial support.

- ¹C. Mogilestue, *Monte Carlo Simulation of Semiconductor Devices* (Chapman and Hall, London, 1993).
- ²M. P. C. M. Krijn, *Semicond. Sci. Technol.* **6**, 27 (1991).
- ³G. C. van der Walle, *Phys. Rev. B* **39**, 1871 (1989).
- ⁴A. Hülsmann, E. Mühlfriedl, B. Raynor, K. Glöser, W. Bronner, K. Köhler, Jo. Schneider, J. Braunstein, M. Schlechtweg, P. Tasker, A. Thiede, and T. Jakobus, *Microelectron. Eng.* **23**, 437 (1994).
- ⁵T. Gonzalez and D. Pardo, *IEEE Trans. Electron Devices* **42**, 605 (1995).
- ⁶M. Berroth and R. Bosch, *IEEE Trans. Microwave Theory Tech.* **38**, 891 (1990).
- ⁷M. Schlechtweg, W. H. Haydl, J. Braunstein, P. J. Tasker, A. Bangert, W. Reinert, L. Verwey, H. Massler, J. Seibel, K. H. Züfle, W. Bronner, T. Fink, A. Hülsmann, P. Hofmann, G. Kaufel, K. Köhler, B. Raynor, and Jo. Schneider, *GaAs IC Symposium*, San Diego, 1995, p. 214 (unpublished).